Journal of Natural Medicines (2021) 75:408–414
https://doi.org/10.1007/s11418-020-01475-w

NOTE

Bisindole alkaloids from *Voacanga grandifolia* leaves

Alfarius Eko Nugroho[1] · Yurika Ono[1] · Eunji Jin[1] · Yusuke Hirasawa[1] · Toshio Kaneda[1] · Abdul Rahman[1] · Idha Kusumawati[2] · Takahiro Tougan[3] · Toshihiro Horii[4] · Noor Cholies Zaini[2] · Hiroshi Morita[1]

Received: 26 October 2020 / Accepted: 7 December 2020 / Published online: 19 January 2021

Abstract

Two new bisindole alkaloids, 12′-*O*-demethyl-vobtusine-5-lactam and isovobtusine-*N*-oxide (**1** and **2**), were isolated from the leaves of *Voacanga grandifolia*, together with two known bisindole alkaloids. Their structures were elucidated on the basis of 1D and 2D NMR data. **1** and **2** showed potent antimalarial activity against *Plasmodium falciparum* 3D7 and very low cytotoxic activity against a human cell line, HepG2 cells.

Graphical abstract

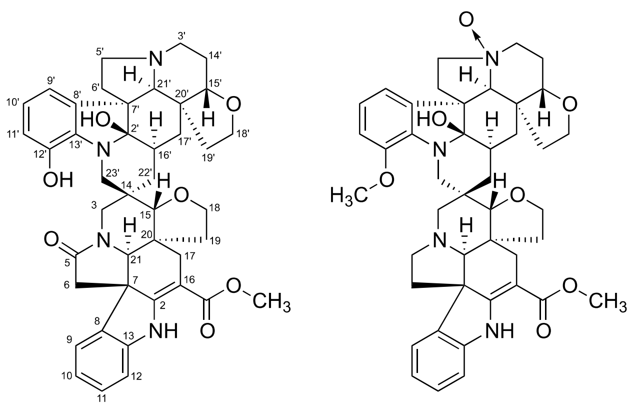

1 **2**

Keywords *Voacanga grandifolia* · Bisindole alkaloids · Apocynaceae · Antimalarial activity

Supplementary Information The online version contains supplementary material available at https://doi.org/10.1007/s11418-020-01475-w.

✉ Hiroshi Morita
moritah@hoshi.ac.jp

[1] Faculty of Pharmaceutical Sciences, Hoshi University, Ebara 2-4-41 Shinagawa-ku, Tokyo 142-8501, Japan

[2] Faculty of Pharmacy, Airlangga University, Jalan Dharmawangsa Dalam, Surabaya 60286, Indonesia

[3] Research Center for Infectious Disease Control, Research Institute for Microbial Diseases, Osaka University, 3-1 Yamadaoka, Suita, Osaka 565-0871, Japan

[4] Department of Molecular Protozoology, Research Institute for Microbial Diseases, Osaka University, 3-1 Yamadaoka, Suita, Osaka 565-0871, Japan

Introduction

Voacanga is a small genus of the Apocynaceae family consisting of 12 species. Species of this genus are distributed mainly in the tropical Africa and Malaysia, and have been reported to contain vobasine, eburnane, iboga, and aspidosperma type of monoterpene indole alkaloids [1]. Various activities have been reported for monoterpene indole alkaloids, such as cytotoxic activity [2–4], anti-melanogenesis [5], anti-plasmodial [6], and vasorelaxant activities [7]. In the search for new bioactive compounds from tropical plants [8–15], alkaloid constituents of *V. grandifolia* leaves were investigated and two new bisindole alkaloids, 12′-*O*-demethyl-vobtusine-5-lactam and isovobtusine-*N*-oxide (**1** and **2**,

Fig. 1), were isolated together with vobtusine-*N*-oxide [16], and vobtusine-3-lactam [17]. The isolation and structure elucidation of **1** and **2** consisting of bis-aspidosperma-type skeleton, from the leaves of *Voacanga grandifolia*, and their antimalarial activities are reported herein.

Results and discussions

Compound **1** {$[\alpha]_D^{24}$ − 117.6° (*c* 1.0, MeOH)} was isolated as an optically active, yellow amorphous solid. The molecular formula was determined by HRESIMS (*m/z* 719.3453 $[M+H]^+$, Δ + 0.8 mmu) as $C_{42}H_{46}N_4O_7$, and the IR absorption at 3340 cm^{-1} and 1715 cm^{-1} indicated the presence of hydroxy and carbonyl groups, respectively. Analysis of the ^1H and ^{13}C NMR data (Table 1) and the HSQC spectrum of **1** revealed the presence of six sp^3 quaternary carbons, five sp^3 methines, fourteen sp^3 methylenes, one methyl, seven sp^2 methines, and nine sp^2 quaternary carbons. Among them, two sp^3 methines (δ_C 63.6; δ_H 2.60, δ_C 64.9; δ_H 3.97) and four sp^3 methylenes (δ_C 44.5; δ_H 2.85 and 4.16, δ_C 44.6; δ_H 3.13 and 4.82, δ_C 48.8; δ_H 2.29 and 2.84, and δ_C 52.0; δ_H 2.21 and 3.02) ascribed to those attached to a nitrogen atom.

The gross structure of **1** was elucidated by analysis of 2D NMR data including the ^1H-^1H COSY, TOCSY, HSQC, and HMBC spectra in $CDCl_3$ (Fig. 2). The ^1H–^1H COSY spectrum revealed the connectivity of seven partial structures **a** (C-9′ ~ C-11′), **b** (C-5′ ~ C-6′), **c** (C-3′, C-14′ ~ C-15′), **d** (C-16′ ~ C-17′, C-22′), **e** (C-18′ ~ C-19′), **f** (C-18 ~ C-19), and **g** (C-9 ~ C-12) as shown in Fig. 2. These partial structures were classified into two units, **a** ~ **e** and **f** ~ **g**.

The connectivity of partial structures **b** and **c** and C-21′ through a nitrogen atom was revealed by the HMBC correlations of H-5′b and H-21′ to C-3′ (δ_C 48.8). The HMBC correlations from H-18′a and H-19′a to C-15′ (δ_C 80.5), H-14′a to C-20′ (δ_C 44.0), and H-19′b to C-17′ (δ_C 32.6) and C-21′ (δ_C 63.6) established the connections among C-15′, C-17′, C-19′, and C-21′ through C-20’.

In addition, HMBC cross peaks of H-6′b to C-8′ (δ_C 134.9), H-9′ to C-21′, H-21′ to C-2′ (δ_C 93.5) and C-6′ (δ_C 31.2), and H-16′ to C-7′ (δ_C 55.9) revealed the connectivity between C-6′, C-16′, C-21′, and an indoline ring. Then, the HMBC correlations of H-23′b and OH-12′ to C-13′ (δ_C 138.2), OH-12′ to C-12′ (δ_C 139.8), and H-22′a and H-23′a to C-2′ suggested the presence of hydroxyl groups at C-2′ and C-12′ in the indoline ring. These NMR data were characteristic of an aspidosperma-type skeleton.

On the other hand, the similar aspidosperma-type skeleton with a methoxy carbonyl at C-16 and a double bond between C-2 and C-16 was suggested by the HMBC correlations in the units **f** and **g** as shown in Fig. 2. The connection of two indole alkaloids through C-14 was revealed by the HMBC correlations from H-23′a to C-14 (δ_C 38.1) and C-22′ (δ_C 35.2) and from H-23′b to C-3 (δ_C 44.5) and C-15 (δ_C 87.8). In particular, the HMBC correlations of H-3a, H_2-6 and H-21 to C-5 (δ_C 172.6) confirmed the presence of a carbonyl at C-5. These data suggested the structure of **1** as 12′-*O*-demethyl-vobtusine-5-lactam.

The relative configuration of each monoterpene indole unit in **1** was assigned by NOESY correlations as shown in computer-generated 3D drawing (Fig. 3). In **1a** (partial structures **a** ~ **e**), the NOESY correlations of H-21′/H-18′a and H-9′, and H-15′/H-18′b and H-17′b suggested that both C-21′ and C-15′ should be *S** and C-7′ and C-20′ should be *R**. The relative configuration of C-2′ (δ_C 93.5) was deduced to be *R** based on the similarity with the chemical shift (δ_C 93.7) of vobtusine [17]. Stereochemistry of H-16′ was elucidated to be α-oriented by $^3J_{H\text{-}16'/H\text{-}17'a}$ (13.0 Hz) and $^3J_{H\text{-}16'/H\text{-}22'b}$ (13.4 Hz), and the NOESY correlations in **1a**. In **1b** (partial structures **f** ~ **g**), H-15 is β-oriented and C-20 should be *R** by the NOESY correlations of H-21/H-18 and H-19a. Stereochemistry of a spiro carbon (C-14) in **1c** should be assigned as *R** by the NOESY correlations, suggesting that the diazaspiro [5.5] undecane ring took a chair-chair conformation, as shown in Fig. 3. Finally, the NOESY correlations and ^1H-^1H coupling constant values suggested the relative configuration of **1** to be, as shown in Fig. 1, the same as vobtusine-3-lactam.

Compound **2** {$[\alpha]_D^{24}$ − 123.6° (*c* 1.0, MeOH)} was isolated as an optically active, yellow amorphous solid. The molecular formula was determined by HRESIMS (*m/z* 735.3765 $[M+H]^+$, Δ 0.7 mmu) as $C_{43}H_{50}N_4O_7$, and the IR absorption at 3340 cm^{-1} and 1685 cm^{-1} indicated the presence of hydroxy and carbonyl groups, respectively. In addition, the ^{13}C NMR data of **2** (Table 1) were similar to those of vobtusine-*N*-oxide and isovobtusine [16,17]. The

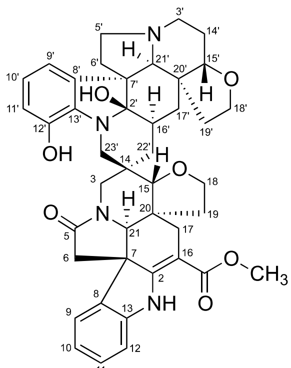

1

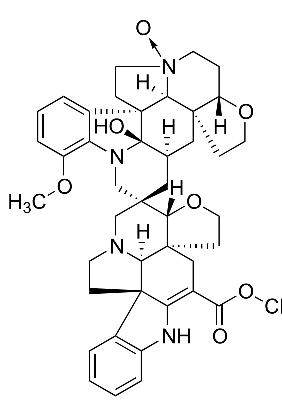

2

Fig. 1 Structures of isolated compounds (**1** and **2**) from *Voacanga grandifolia*

Table 1. ^{1}H (600 MHz) and ^{13}C (150 MHz) NMR data of **1** and **2** in $CDCl_3$

	1		**2**	
	δ_H (*J*, Hz)	δ_C	δ_H (*J*, Hz)	δ_C
2		164.4		167.5
3a	4.16 (1H, d, 13.0)	44.5	2.68 (1H, d, 10.8)	58.2
3b	2.85 (1H, d, 13.0)		2.64 (1H, d, 10.8)	
5a		172.6	2.89 (1H, m)	51.5
5b			2.74 (1H, m)	
6a	2.97 (1H, d, 18.0)	48.3	2.01 (1H, m)	44.4
6b	2.65 (1H, d, 18.0)		1.70 (1H, m)	
7		47.4		55.1
8		135.7		138.1
9	7.12 (1H, d, 7.5)	121.2	7.20 (1H, d, 7.2)	121.7
10	6.94 (1H, dd, 7.6, 7.5)	121.8	6.87 (1H, dd, 7.6, 7.2)	120.7
11	7.21 (1H, dd, 7.8, 7.6)	129	7.12 (1H, dd, 7.7, 7.6)	127.7
12	6.86 (1H, d, 7.8)	109.8	6.77 (1H, d, 7.7)	109.3
13		142.9		143
14		38.1		39.2
15	3.42 (1H, s)	87.8	3.17 (1H, s)	81.8
16		94		94.5
17a	2.52 (1H, s)	26.1	2.81 (1H, d, 13.8)	28.5
17b	2.52 (1H, s)		2.20 (1H, d, 13.8)	
18a	3.72 (1H, m)	63.9	3.65 (1H, m)	63.6
18b	3.72 (1H, m)		3.30 (1H, m)	
19a	1.56 (1H, m)	35.9	1.26 (1H, m)	35
19b	1.39 (1H, ddd, 13.0, 7.9, 4.8)		1.17 (1H, m)	
20		46.5		47.9
21	3.97 (1H, s)	64.9	2.83 (1H, s)	70
CO		168		168.4
OMe	3.80 (3H, s)	51.4	3.71 (3H, s)	51
2’		93.5		92.3
3′a	2.84 (1H, m)	48.8	3.45 (1H, m)	58.7
3′b	2.29 (1H, m)		3.45 (1H, m)	
5′a	3.02 (1H, m)	52	3.52 (1H, m)	67.2
5′b	2.21 (1H, m)		3.32 (1H, m)	
6′a	2.79 (1H, m)	31.2	3.58 (1H, m)	30.7
6′b	1.24 (1H, m)		1.36 (1H, m)	
7’		55.9		55.6
8’		134.9		133.6
9’	6.74 (1H, d, 7.3)	116	6.64 (1H, d, 7.6)	111.1
10’	6.61 (1H, dd, 7.3, 7.2)	119.1	6.62 (1H, dd, 7.6, 7.6)	118.1
11’	6.72 (1H, d, 7.2)	121.6	6.59 (1H, d, 7.6)	112.5
12’		139.8		146.3
13’		138.2		137.7
14′a	1.95 (1H, br d, 12.0)	25.8	2.92 (1H, m)	22.8
14′b	1.86 (1H, m)		2.01 (1H, m)	
15’	3.44 (1H, br s)	80.5	3.66 (1H, dd, 2.9, 2.9)	78.7
16’	1.87 (1H, m)	31.6	2.03 (1H, m)	33.9
17′a	1.78 (1H, dd, 13.0, 13.0)	32.6	2.56 (1H, dd, 12.5, 12.5)	33.7
17′b	0.86 (1H, br d, 13.0)		0.91 (1H, br d, 12.5)	
18′a	4.05 (1H, m)	65.4	3.98 (1H, m)	65
18′b	3.90 (1H, m)		3.90 (1H, m)	

Table 1. (continued)

	1		2	
	δ_H (*J*, Hz)	δ_C	δ_H (*J*, Hz)	δ_C
19′a	2.35 (1H, m)	36.5	2.48 (1H, ddd, 12.5, 8.1, 3.9)	39.7
19′b	1.52 (1H, m)		1.69 (1H, m)	
20’		44.0		45.4
21’	2.60 (1H, s)	63.6	3.56 (1H, s)	75.3
22′a	1.48 (1H, br d, 13.6)	35.2	2.00 (1H, m)	35
22′b	2.13 (1H, dd, 13.6, 13.4)		2.00 (1H, m)	
23′a	4.82 (1H, d, 14.5)	44.6	4.69 (1H, d, 14.1)	46.7
23′b	3.13 (1H, d, 14.5)		3.02 (1H, d, 14.1)	
12′-OH	6.22 (1H, s)			
12′-OMe			3.75 (3H, s)	54.9

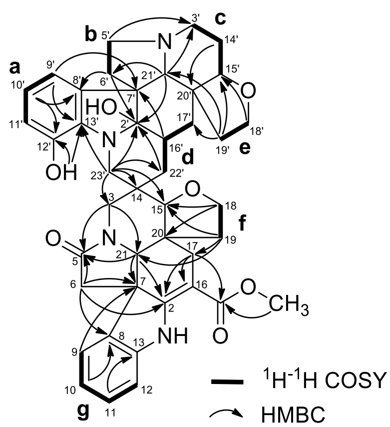

Fig. 2 Selected 2D NMR correlations of **1**

chemical shift differences between **2** and vobtusine-*N*-oxide (i.e. C-3, C-14, C-15, C-18, C-16′, C-22′ and C-23′) suggested **2** to be the 14-*epi* derivative of vobtusine-*N*-oxide, isovobtusine-*N*-oxide, and the downfield shifts of signals ascribed to C-3′, C-5′ and C-21′ in **2** relative to isovobtusine further supported this conclusion.

Biological activity of 1 and 2

The antimalarial activity and cytotoxic activity of **1** and **2** were evaluated in vitro. Against *P. falciparum* 3D7 strain, **1** and **2** showed potent antimalarial activity [Table 2: half-maximal (50%) inhibitory concentration (IC_{50}) = 5.1 and 3.3 μM, respectively]. Chloroquine was used as a positive control (IC_{50} = 0.026 μM). In contrast, the cytotoxic activity of both **1** and **2** was low [Table 2: half-maximal (50%) cytotoxic concentration (CC_{50}) ≧ 50 μM] against the human cell line, HepG2 cells.

Experimental section

General experimental procedures

Optical rotations were measured on a JASCO DIP-1000 polarimeter, UV spectra on a Shimadzu UVmini-1240 spectrophotometer, and IR spectra on a JASCO FT/IR-4100 spectrophotometer. High-resolution ESI MS were obtained on a JMS-T100LP (JEOL). ^{1}H and 2D NMR spectra were measured on a 600 MHz spectrometer at 300 K, and ^{13}C NMR spectra on a 150 MHz spectrometer. Residual solvent chemical shifts were used as internal standard, δ_H 7.26 and δ_C 77.0 for $CHCl_3$. Standard pulse sequences were used for the 2D NMR experiments.

Material

The leaves of *V. grandiflora* were collected at the Purwodadi Botanical Garden in March 2008. The botanical identification was made by Ms. Sri Wuryanti, Purwodadi Botanical Garden. A voucher specimen has been deposited in the herbarium at Purwodadi Botanical Garden, Pasuruan, Indonesia.

Extraction and isolation

Finely powdered leaves of *V. grandiflora* (400 g) were extracted with MeOH (1L × 3) at room temperature. The combined extracts were evaporated under reduced pressure to give a residue (30 g). The extract was dissolved in 3% aqueous tartaric acid (pH 2) and then partitioned with EtOAc. The aqueous layer was treated with Na_2CO_3 to pH 9 and was partitioned successively by $CHCl_3$ and *n*-BuOH. The $CHCl_3$ soluble materials (3.9 g) was subjected to an LH-20 column ($CHCl_3$/MeOH, 1:1) to obtain ten fractions.

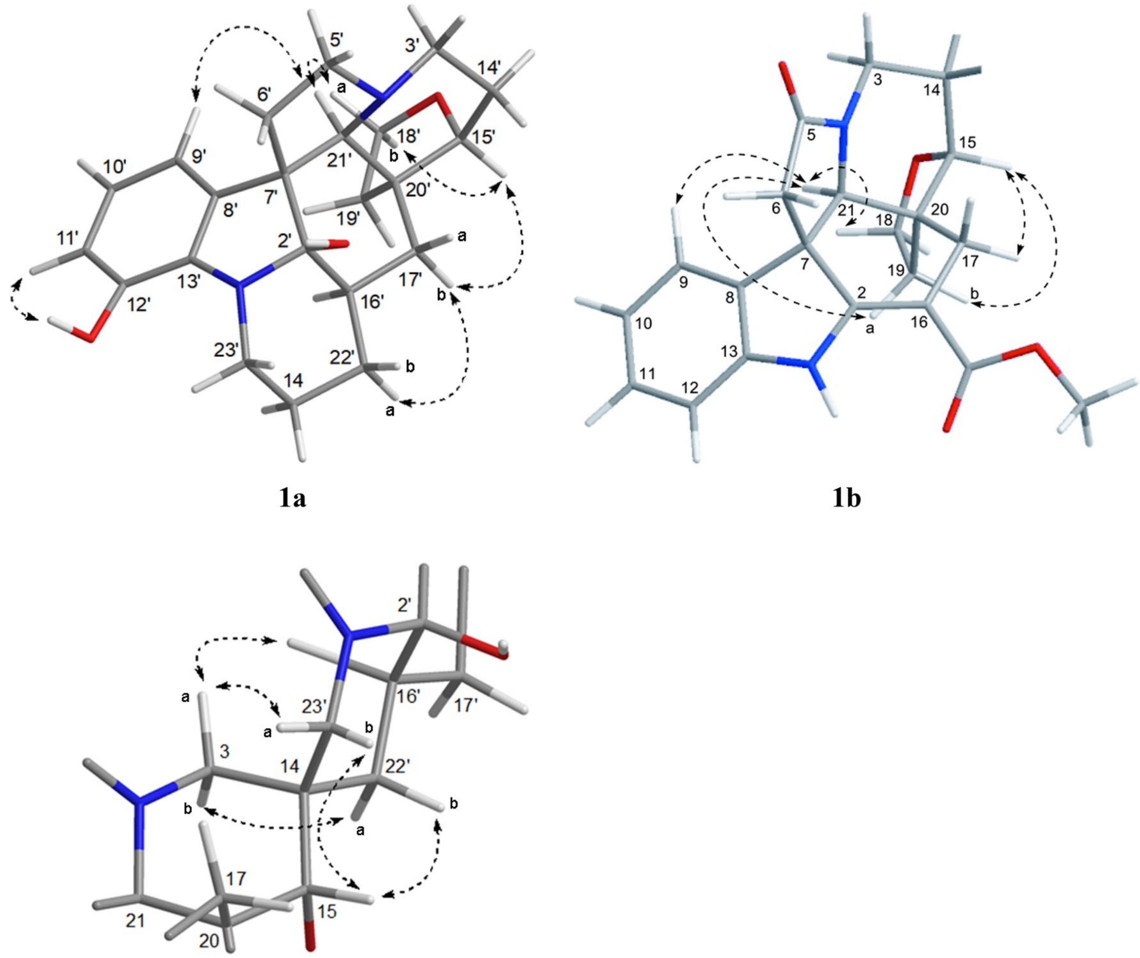

Fig. 3 Selected NOESY correlations of **1**

Table 2 Antimalarial and cytotoxic activities of **1** and **2** against *Plasmodium falciparum* 3D7

	Antimalarial acitivity	Cytotoxic activity
Compound	IC_{50} (μM)	CC_{50} (μM)
1	5.1	> 50
2	3.3	> 50

Fraction 7 (360 mg) was fractionated by silica gel column chromatography ($CHCl_3$/MeOH, 0:1 → 1:0), ODS column chromatography (MeOH/H_2O) and RP-HPLC (Nacalai tesque Cholester, 10 × 250 mm; 24% MeCN in 0.1% aqueous HCO_2H; flow rate 3.5 mL/min; UV detection at 254 nm) to obtain 1 (1.5 mg, 0.0004%), 2 (1.5 mg, 0.0004%), vobtusine-*N*-oxide (1.9 mg, 0.0005%) [16], and vobtusine-3-lactam (0.8 mg, 0.0002%) [17].

12′-demethyl-vobtusine-5-lactam (**1**): Yellow amorphous solid; [α] -117.6 (*c* 1.0, MeOH); IR (film) ν_{max} 3340 and 1715 cm^{-1}; UV/Vis λ_{max} (MeOH) nm (log *ε*): 306 (3.57), 273 (3.84), 227 (4.41) and 206 (4.41) nm; ESIMS (pos.) *m*/*z* 719 $(M+H)^+$; HRMS-ESI: *m*/*z* $[M+H]^+$ calcd for $C_{42}H_{47}N_4O_7$: 719.3445; found 719.3453.

Isovobtusine-*N*-oxide (**2**): Yellow amorphous solid; [α] -123.6 (*c* 1.0, MeOH); IR (film) ν_{max} 3370 and 1685 cm^{-1}; UV/Vis λ_{max} (MeOH) nm (log ε): 328 (4.22), 299 (4.16), 259 (3.93) and 220 (4.47) nm; ESIMS (pos.) *m*/*z* 735 $(M+H)^+$; HRMS-ESI: *m*/*z* $[M+H]^+$ calcd for $C_{43}H_{51}N_4O_7$: 735.3758; found 735.3765.

Parasite culture

P. falciparum laboratory strain 3D7 was obtained from Prof. Masatsugu Kimura (Osaka City University, Osaka, Japan). For the assessment of antimalarial activity of the compounds in vitro, the parasites were cultured in Roswell Park

Memorial Institute (RPMI) 1640 medium supplemented with 0.5 g/L L-glutamine, 5.96 g/L HEPES, 2 g/L sodium bicarbonate ($NaHCO_3$), 50 mg/L hypoxanthine, 10 mg/L gentamicin, 10% heat-inactivated human serum, and red blood cells (RBCs) at a 3% hematocrit in an atmosphere of 5% CO_2, 5% O_2, and 90% N_2 at 37 °C as previously described [18]. Ring-form-infected RBCs were collected using the sorbitol synchronization technique [19]. Briefly, the cultured cells were collected by centrifugation at 840 g for 5 min at room temperature, suspended in a fivefold volume of 5% D-sorbitol (Nacalai Tesque, Kyoto, Japan) for 10 min at room temperature, and then they were washed twice with RPMI 1640 medium to remove the D-sorbitol. The utilization of blood samples of healthy Japanese volunteers for the parasite culture was approved by the institutional review committee of the Research Institute for Microbial Diseases (RIMD), Osaka University (approval number: 22–3).

Antimalarial activity

Ring-form-synchronized parasites were cultured with compounds **1** and **2** at sequentially decreasing concentrations (50, 15, 5, 1.5, 0.5, 0.15, 0.05, and 0.015 µM) for 48 h for the flow cytometric analysis using an automated hematology analyzer, XN-30. The XN-30 analyzer was equipped with a prototype algorithm for cultured falciparum parasites [prototype; software version: 01–03, (build 16)] and used specific reagents (CELLPACK DCL, SULFOLYSER, Lysercell M, and Fluorocell M) (Sysmex, Kobe, Japan) [20,21]. Approximately 100 µL of the culture suspension diluted with 100 µL phosphate-buffered saline was added to a BD Microtainer MAP Microtube for Automated Process K2 EDTA 1.0 mg tube (Becton Dickinson and Co., Franklin Lakes, NJ, USA) and loaded onto the XN-30 analyzer with an auto-sampler as described in the instrument manual (Sysmex). The parasitemia shown as MI-RBC% was automatically reported [20]. Then 0.5% DMSO alone or containing 5 µM artemisinin used as the negative and positive controls, respectively. The growth inhibition (GI) rate was calculated from the MI-RBC% according to the following equation:

$$\mathrm{GI}(\%) = 100 - (\text{test sample} - \text{positive control}) / (\text{negative control} - \text{positive control}) \times 100$$

The IC_{50} was calculated from GI (%) using GraphPad Prism version 5.0 (GraphPad Prism Software, San Diego, CA, USA) [22].

Cytotoxic activity

HepG2 (JCRB1054) cell line was obtained from the Japanese Collection of Research Bioresources (JCRB, Osaka, Japan). The cells were cultured in Dulbecco's modified Eagle's medium [DMEM (1.0 g/L glucose) with L-glutamine and sodium pyruvate; Nacalai Tesque, Kyoto, Japan] supplemented with 10% (v/v) fetal bovine serum (FBS; Gibco-BRL, Grand Island, NY, USA) in a humidified incubator with 5% CO_2 at 37 °C. For the assay, the cells (5×10^3/well) were seeded in a 96-well plate. **1** and **2** at gradually decreasing concentrations (50, 15, 5, 1.5, 0.5, 0.15, 0.05, and 0.015 µM) were added to the cell culture after 24 h and the cells were subsequently cultured for 48 h. Cell viability was measured using a Cell Counting Kit-8 (Dojindo, Kumamoto, Japan) according to the manufacturer's instructions. Briefly, 10 µL CCK-8 reagent was added to each well containing culture medium and incubated for 2 h under standard culture conditions. The absorbance of the sample was measured at 450 nm using a PowerWave HT microplate spectrophotometer (BioTek Instruments, Winooski, VT, USA). The cell viability was expressed as a percentage of the absorbance of the untreated control cells after subtracting the appropriate background intensity. The CC_{50} was calculated from the cell viability using GraphPad Prism version 5.0.

Acknowledgment We thank Prof. Masatsugu Kimura (Osaka City University, Osaka, Japan) for the kind gift of the 3D7 strain. We also thank Mr. Yuji Toya and Dr. Kinya Uchihashi (Sysmex, Kobe, Japan) for the setting of the XN-30 analyzer and Ms. Toshie Ishisaka and Ms. Sawako Itagaki for their technical assistance. This work was supported by JSPS KAKENHI Grant Number JP19K07152 to MH and partially supported by Sysmex Corporation to TT.

References

1. Macabeo APG, Alejandro GJD, Hallare AV, Vidar WS, Villaflores OB (2009) Phytochemical Survey and Pharmacological Activities of the Indole Alkaloids in the Genus Voacanga Thouars (Apocynaceae) - An Update. Phcog Rev 3:132-142
2. Hirasawa Y, Shoji T, Arai T, Nugroho AE, Deguchi J, Hosoya T, Uchiyama N, Goda Y, Awang K, Hadi AHA, Shiro M, Morita H (2010) Bisleuconothine a, an eburnane-aspidosperma bisindole alkaloid from *Leuconotis griffithii*. Bioorg Med Chem Lett 20:2021–2024
3. Haseo A, Nugroho AE, Hirasawa Y, Kaneda T, Shirota O, Rachman A, Kusumawati I, Zaini NC, Morita H (2015) A new indole alkaloids from *Voacanga grandifolia*. Heterocycles 90:601–606
4. Wong CP, Seki A, Horiguchi K, Shoji T, Arai T, Nugroho AE, Hirasawa Y, Sato F, Kaneda T, Morita H (2015) Bisleuconothine a induces autophagosome formation by interfering with AKT-mTOR signaling pathway. J Nat Prod 78:1656–1662
5. Koyama K, Hirasawa Y, Hosoya T, Hoe TC, Chan K-L, Morita H (2010) Alpneumines A-H, new anti-melanogenic indole alkaloids from *Alstonia pneumatophora*. Bioorg Med Chem 18:4415–4421
6. Nugroho AE, Sugai M, Hirasawa Y, Hosoya T, Awang K, Hadi AHA, Ekasari W, Widyawaruyanti A, Morita H (2011) New antiplasmodial indole alkaloids from *Hunteria zeylanica*. Bioorg Med Chem Lett 21:3417–3419
7. Hirasawa Y, Hara M, Nugroho AE, Sugai M, Zaima K, Kawahara N, Goda Y, Awang K, Hadi AHA, Litaudon M, Morita H (2010) Bisnicalaterines B and C, atropisomeric bisindole alkaloids from

hunteria zeylanica, showing vasorelaxant activity. J Org Chem 75:4218–4223
8. Nugroho AE, Hashimoto A, Wong CP, Yokoe H, Tsubuki M, Kaneda T, Hadi AHA, Morita H (2018) Ceramicines M-P from *Chisocheton ceramicus*: isolation and structure–activity relationship study. J Nat Med 72:64–72
9. Nugroho AE, Inoue D, Wong CP, Hirasawa Y, Kaneda T, Shirota O, Hadi AHA, Morita H (2018) Reinereins A and B, new onocerane triterpenoids from *Reinwardtiodendron cinereum*. J Nat Med 72:588–592
10. Kaneda T, Matsumoto M, Sotozono Y, Fukami S, Nugroho AE, Hirasawa Y, Hamid AHA, Morita H (2019) Cycloartane triterpenoid (23R, 24E)-23-acetoxymangiferonic acid inhibited proliferation and migration in B16–F10 melanoma via MITF downregulation caused by inhibition of both β-catenin and c-Raf–MEK1–ERK signaling axis. J Nat Med 73:47–58
11. Tang Y, Nugroho AE, Hirasawa Y, Tougan T, Horii T, Hamid AHA, Morita H (2019) Leucophyllinines A and B, Bisindole alkaloids from *Leuconotis eugeniifolia*. J Nat Med 73:533–540
12. Amelia P, Nugroho AE, Hirasawa Y, Kaneda T, Tougan T, Horii T, Morita H (2019) Indole alkaloids from *Tabernaemontana macrocarpa* Jack. J Nat Med 73:820–825
13. Hirasawa Y, Dai X, Deguchi J, Hatano S, Ohtsuka R, Nugroho AE, Kaneda T, Morita H (2019) New Vasorelaxant Indole Alkaloids, Taberniacins A and B, from *Tabernaemontana divaricata*. J Nat Med 73:627–632
14. Prema WCP, Awouafack MD, Nugroho AE, Win YY, Win NN, Ngwe H, Morita H, Morita H (2019) Two new quassinoids and other constituents from the *Picrasma javanica* wood and their biological activities. J Nat Med 73:589–596
15. Prema WCP, Kodama T, Nugroho AE, El-Desoky AH, Awouafack MD, Win YY, Ngwe H, Abe I, Morita H, Morita H (2020) Three new quassinoids isolated from the wood of *Picrasma javanica* and their anti-Vpr activities. J Nat Med 74:571–578
16. Agwada VC, Naranjo J, Hesse M, Schmid H, Rolland Y, Kunesch N, Poisson J, Chatterjee A (1977) Die struktur des bisindolalkaloides amatain (= grandifolin, subsessilin). Helv Chim Acta 60:2830–2853
17. Rolland Y, Kunesch N, Poisson J, Hagaman EW, Schell FM, Wenkert E (1976) *Voacanga* alkaloids. 16. Carbon-13 nuclear magnetic resonance spectroscopy of naturally occurring substances. 43. Carbon-13 nuclear magnetic resonance analysis of bis-indoline alkaloids of two *Voacanga* species. J Org Chem 41:3270–3275
18. Trager W, Jensen JB (1976) Human malaria parasites in continuous culture. Science 193:673–675
19. Lambros C, Vanderberg JP (1979) Synchronization of Plasmodium falciparum erythrocytic stages in culture. J Parasitol 65:418–420
20. Tougan T, Suzuki Y, Itagaki S, Izuka M, Toya Y, Uchihashi K, Horii T (2018) An automated haematology analyzer XN-30 distinguishes developmental stages of falciparum malaria parasite cultured in vitro. Malar J 17:59
21. Toya T, Tougan T, Horii T, Uchihashi K (2021) Lysercell M enhances the detection of stage-specific Plasmodium-infected red blood cells in the automated hematology analyzer XN-31 prototype. Parasitol Int 80:102206. https://pubmed.ncbi.nlm.nih.gov/33049417/
22. Tougan T, Toya Y, Uchihashi K, Horii T (2019) Application of the automated haematology analyzer XN-30 for discovery and development of anti-malarial drugs. Malar J 18:8